Indian Journal of Drugs, 2020, 8(2), 33-53 **ISSN: 2348-1684**
Research Article

FORMULATION AND DEVELOPMENT OF NANOPARTICLES WITH MANNOSE-6-PHOSPHATE COATING FOR THE TREATMENT OF LIVER CIRRHOSIS

Sahani Vandana*

Department of Pharmaceutics, Division of Pharmaceutical sciences, Shree dev bhoomi institute of education science and technology, Dehradun.

***For Correspondence:**
Department of Pharmaceutics, Division of Pharmaceutical sciences, Shree dev bhoomi institute of education science and technology, Dehradun.

Received: 26.03.2020
Accepted: 22.06.2020

Access this article online

Website:
www.drugresearch.in

Quick Response Code:

ABSTRACT

Cirrhosis is one of the chronic generalised disease and has a variety of clinical manifestations and complications some of which can be a life threatening. This results in decrease in hepatocellular mass and thus functions. It is 12th leading cause of death in United States. Hepatic stellate cells (HSC) plays a crucial role in the development of liver fibrosis because of their prominent role in extracellular matrix production, regulation of vascular tone, and production of inflammatory mediators such as transforming growth factor-b (TGF-b) and platelet-derived growth factor (PDGF). Therefore, these cells are major target for the treatment of Cirrhosis. Cell-specific delivery can provide a solution to these problems, but a specific drug carrier for HSC has not been described until now. The mannose 6-phosphate/insulin-like growth factor II (M6P/IGF-II) receptor, which is expressed in particular upon HSC during fibrosis, may serve as a target-receptor for a potential carrier. Carrier molecules are designed for their selective cellular uptake, taking advantage of specific receptors or binding sites present on the surface membrane of the target cell. In the present study, an attempt was made to develop mannose coated albumin nanoparticles of Ursodeoxycholic acid for treatment of Cirrhosis. By developing the mannose coated nanoparticulated delivery of Ursodeoxycholic acid the required action of drug at the target site i.e. at liver can be provided. The advantage of targeting helps to reduce the systemic side effects which may be due to the distribution of the drug to the other organs and thus helps in maintaining the required concentration at the desired site. Moreover, as nanoparticles have higher carrier capacity, helps to provide the sustain action and thus reduce the dose frequency and increase the patient compliance. The use of ursodeoxycholic acid in the treatment of Cirrhosis disease was as a hepatoprotective which helps in the treatment of Cirrhosis disease. In the current work, we had prepared mannose coated albumin nanoparticles using desolvation method. The coating of nanoparticles with mannose helps to get binds the nanocarrier with the receptors present in hepatocytes. Thus, the developed formulations overcome the drawback and limitation of the conventional drug delivery systems.

KEY WORDS: Liver, Cirrhosis, Hepatic stellate cells targeting.

INTRODUCTION

Liver Cirrhosis is the end stage of all the diseases like viral hepatitis, alcohol abuse, non-alcoholic steatohepatitis and other diseases [1]. In Liver Cirrhosis acute liver damage leads to chronic inflammation and fibrosis. Unfortunately, there is no treatment currently available for liver fibrosis apart from organ transplantation but in that also donor organ shortage and high costs remain a serious problem. Hepatic failure after transplantation is still burdened by a high mortality rate.So finding a proper pharmacotherapeutic treatment for the liver fibrosis is very challenging.[6] Selective targeting of anti-fibrotic drugs to hepatic stellate cells (HSC) has recently been proposed which are identified as the key fibrogenic cell type in the progression of Cirrhosis[2, 3, 4]. With the help of targeted drug delivery system potent antifibrotic drug can be delivered intracellular within the diseased liver and even within the desired cell type. For this mannose-6-phosphate modified albumin

(M6PHSA) has been proposed which binds with high affinity to the insulin-like growth factor II/mannose-6-phosphate receptor on activated HSC [5].

Hepatic stellate cells

Hepatic stellate cells are located in the sub endothelial space, between the basolateral surface of hepatocytes and the anti-luminal side of sinusoidal endothelial cells.They comprise approximately one-third of the nonparenchymal cell population and 15% of the total number of resident cells in normal liver. Stellate cells in normal liver have spindle-shaped cell bodies with oval or elongated nuclei [20]. Ultra structurally, there have moderately developed rough endoplasmic reticulum (rER), juxtanuclear small Golgi complex, and prominent dendritic cytoplasmic processes. The sub endothelial processes wrap around sinusoids between endothelial cells and hepatocytes. On each of these processes, there are numerous thorny micro projections (spines). [7,10,11] The function of these projections had been obscure until a recent, elegant study has demonstrated that these protrusions serve a vital role as the cell's leading edge in "sensing" chemotactic signals, and then transmitting them to the cell's mechanical apparatus to generate a contractile force.A single stellate cell usually surrounds more than two nearby sinusoids. On the other side of the cell (i.e. the anti-luminal surface), multiple processes extend across the space of Disse to make contact with hepatocytes.This intimate contact between stellate cells and their neighbouring cell types may facilitate intercellular transport of soluble mediators and cytokines.In addition, stellate cells are directly adjacent to nerve endings which are consistent with reports identifying neurotrophin receptors and with functional studies confirming neurohumoral responsiveness of stellate cells.[17] The most characteristic feature of stellate cells in normal liver is their cytoplasmic storage of vitamin (retinoid) droplets. The number of droplets varies with the species and the abundance of vitamin A stores of the organism. During liver injury, the fine structure of stellate cells changes considerably. They lose their characteristic droplets and become "activated". The rER becomes enlarged, accompanied with a well-developed Golgi apparatus, suggesting active protein synthesis.Bundles of numerous microfilaments appear beneath the cell membrane.The activated stellate cells then evolve into myofibroblast-like cells with newly formed collagen fibrils surrounding them.[19,16]

M6PHSA as a soluble carrier protein

Albumin is the most abundant plasma protein, and has a biological half-life of 19 days.It consists of a single chain of 585 amino acids organized in a tri dimensional structure in a helical conformation. The helices are bound by 17 di-sulphide bridges, leaving only one free thiol (Cys34) [8,12]. Albumin is biodegradable and therefore biocompatible and contains many different functional groups, i.e. -NH_2 of the lysine residues or methionine, which can be used for conjugation of the homing device, the linker, or the drug.In addition, due to its size and charge, it is not cleared from the blood by renal filtration. [13] In our strategy, albumin was modified with sugar mannose-6-phosphate groups on its surface resulting in M6PHSA. M6PHSA has been shown to specifically interact with mannose 6-phosphate/insulin-like growth factor II (M6P/IGFII) receptors expressed on the surface of hepatic stellate cells.Due to stellate cell proliferation during liver fibrosis and a concomitant increase in M6P/IGF II receptor expression on this cell type [9,18], the disease process itself may selectively direct the carriers to the diseased tissue. [14,15] This targeting strategy may largely contribute to the increased therapeutic concentration of drug in the target tissue.

MATERIAL AND METHODS

Drug: Ursodeoxycholic acid (UDCA/Ursidol)

Chemical Formula: 3α,7β-dihydroxy-5β-cholan-24-oicacid OR (*R*)-4-((3*R*,5*S*,8*R*,9*S*,10*S*,13*R*,14*S*,17*R*)-3,7-dihydroxy-10,13-dimethylhexadecahydro-1h-cyclopenta[a]phenanthrene-17-yl)pentanoic acid

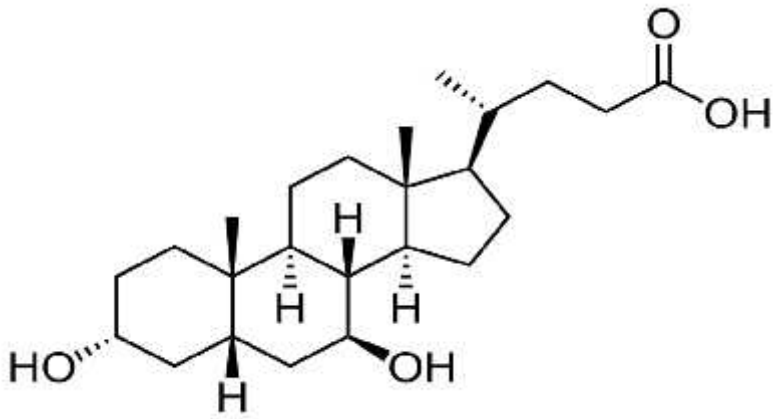

Empirical Formula: $C_{24}H_{40}O$
Molecular weight: 392.57
Description: white or almost white powder, odourless and bitter in taste.
Melting point: 203℃ (397℉)
Solubility: Low soluble in water, freely soluble in ethanol and methanol. Water solubility is 20 mg/l at20℃.
Therapeutic activity: anticolelithic and hepatoprotective.
Mechanism of action:
Drug acts mainly by three ways.

- Protection of cholangiocystis against cytotoxicity of hydrophobic bile acids (anticholethacic).
- Simulation of hepato-biliary secretion via ca^{+2} / protein kinase pathway.
- Protection of hepatocytes against bile induced hepatocytes against bile induced apoptosis.

Indication and Dosage:

- For Primary biliary Cirrhosis- 10-15mg/Kg daily in 2-4 divided dose.
- For prophylaxis of gall stone- 300 mg twice a day.
- For dissolution of Cholestrol rich gall stone-6-12 mg/Kg daily as single dose at bed time or in 2-3 divided dose, continued for 3-4 months.

Brand name: Udihep (Win-medicare), Livo-kind (Mankind), Udiliv (Abott), Golbi (Intas)
Imp note:

- Drug is not recommended in children.
- FDA approved drug to be treat Primary biliary Cirrhosis.

Bovine Serum Albumin (BSA)
Molecular weight – 66,430
BSA is a single polypeptide chain consisting of about 583 amino acid residues and no carbohydrates.Albumins are a group of proteins which occur plentifully in the body fluids and tissues of mammals and in some plant seeds. Unlike globulins, albumins have comparatively low molecular weights are soluble in water, are easily crystallized, and contain an excess of acidic amino acids. Serum and plasma albumin is carbohydrate-free and comprises 55-62% of the protein present.**Storage:** 2-8℃.
Sodium Chloride
Sodium Chloride, also known as salt, common salt, table salt or halite is an ionic compound with the formula NaCl, representing equal proportions of sodium and chloride. Sodium Chloride is the salt most responsible for the salinity of the ocean and extracellular fluid of many multicellular organisms. As the major ingredient in edible salt, it is commonly used as a condiment and food preservative.
Glutaraldehyde
Glutaraldehyde is a pungent colourless liquid which when heated to decomposition emits acrid smoke. It is soluble in water, alcohol,benzene and ether and is volatile in steam. Glutaraldehydepolymerizes in water to glassy foam.

Fig 4.2: Structure of Glutaraldehyde

Uses:

- It is registered as an antimicrobial and as a bactericide, a fungicide and a virucide. It is used to sterilize and disinfect hospital and veterinary equipment and to disinfect surfaces in hospitals, veterinary hospitals, nursing homes and food processing plants.
- It is used to cross link the proteins.

Mannose-6-Phosphate

Mannose-6-phosphate (M6P) is a molecule bound by lectin in the immune system. M6P is converted to fructose 6-phosphate by mannose phosphate isomerase.M6P is a key targeting signal for acid hydrolase precursor proteins that are destined for transport to lysosomes. The M6P tag is added to such proteins in the cis-Golgi apparatus. Specifically, in a reaction involving uridinediphosphate (UDP) and N-acetylglucosamine, the enzyme N-acetylglucosamine-1-phosphate transferasecatalyzes the N-linked glycosylation of asparagine residues with M6P. Once appropriately marked with the M6P targeting signal, these proteins are moved to the trans-Golgi network. There, the M6P moiety is recognized and bound by mannose 6-phosphate receptor (MPR) proteins at pH 6.5-6.7.

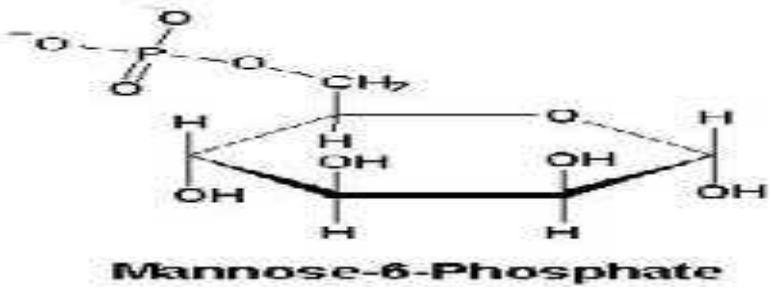

Fig 4.3: Structure of Mannose-6-Phosphate

Table 5.1 : List of chemicals used with supplier

S. No.	Materials	Manufacturer
1	Ursodeoxycholic acid	Windlas Biotech Ltd, Dehradun
2	Bovine Serum Albumin	Central Drug House Ltd, New Delhi
3	Sodium Chloride	Central Drug House Ltd, New Delhi
4	Ethanol	Central Drug House Ltd, NewDelhi
5	Glutaraldehyde	Central Drug House Ltd, NewDelhi
6	Mannose-6-Phosphate	Central Drug House Ltd, NewDelhi

Table5.2: List of instrument used

S. No.	Instrument	Manufacturer
1.	Electronic Balance	Shimadzu Corporation,Japan
2.	Magnetic Balance	Hicon Grover Enterprises, India
3.	Distillation Assembly	Gupta Scientific,Ambala,India
4.	Fourier Transform Infrared (FTIR) Spectrometer	Perkin Elemer Spectrum Two, India
5.	Double beam UV spectrometer	Elico SL 210,India
6.	pH Analyzer	Elico,India
7.	Sonicator	Sonar, India
8.	Centrifuge	RemiEquipments Ltd, Mumbai,India
9.	SEM(Scanning Electron Microscope)	Zeiss, Evo 40, India

1. Preformulation Studies

Preformulation testing is the first step in the rational development of dosage forms of a drug. It can be defined as the investigation of physical and chemical properties of drug substance alone or in combination with excipients.The overall objective of preformulation studies is to generate information useful to formulator in developing stable and bioavailable dosage forms which can be mass produced**.**

1.1 Identification tests

1.1.1. Identification of drug by FTIR:

Infrared spectrum of Ursodeoxycholic acid was determined by using Fourier Transform Infrared Spectrophotometer using KBr disks method. The sample (0.5 to 1.0 mg) is finely grounded and intimately mixed with approximately 100 mg of dry potassium bromide powder. Grinding and mixing can be done with mortar and pestle. The mixture is then pressed into a transparent disk in an evacuable die at sufficiently high pressure. Suitable KBr disks or pellets can often be made using a simpler device such as a hydraulic press. The base line correction was done using dried potassium bromide. Thenthe spectrum of dried mixture of drug and potassium bromide was scanned from 4000 cm^{-1} to 400 cm^{-1}.

1.1.2. Organoleptic characteristics:

The colour,odour and taste of the drug were characterized and recorded.

1.1.3.Solubility:

The solubility of the drug were checked in different solvents like distilled water,buffers,ethanol and organic solvents and recorded. This might be helpful in selection of a suitable solvent to dissolve drug as well as excipients used in formulations.

Table : Descriptive terminology for Solublility

S.No.	Descriptive term	Parts of Solvent required for Part of Solute
1.	Very soluble	Less than 1
2.	Freely soluble	From 1 to 10
3.	Soluble	From 10 to 30
4.	Sparingly solublesoluble	From 30 to 100
5.	Slightly soluble	From 100 to 1000
6.	Very slightly soluble	From 1000 to 10,000
7.	Practically insoluble, or Insoluble	10,000 or more

1.1.4. Melting Point determination:

The sample was loaded into a sealed capillary (melting point capillary) which was then placed in the melting point apparatus. The sample is then heated & as the temperature increases, the sample was observed to detect the phase change from solid to liquid phase. The temperature at which this phase change occurs gives the melting point.

1.2. Spectral Studies

1.2.1. Drug - excipient Compatibility Study:

Drug and polymer was mixed in the equal ratio and finally grounded and intimately mixed with approximately 100 mg of dry potassium bromide powder. Grinding and mixing can be done with mortar and pestle. The mixture is then pressed into a transparent disk in an evacuable die at sufficiently high pressure. Suitable KBr disks or pellets can often be made using a simpler device such as a hydraulic press. The base line correction was done using dried potassium bromide. Then,the spectrum of dried mixture of drug and potassium bromide was scanned from 4000cm^{-1} to 400 cm^{-1}.

1.2.2. Preparation of Calibration Curve of Ursodeoxycholic acid

a.Determination of λ_{max} of Ursodeoxycholic acid

Methanol and distilled water was investigated to develop a suitable UV-spectrophotometric method for the analysis of Ursodeoxycholic acid in formulations. For selection of media the criteria employed were sensitivity,ease of sample preparations,solubility of drug,and cost of solvents and applicability of method to various purposes.An UV spectroscopic scanning run (200-400nm) was carried out .The analysis was carried out using Distilled water as blank. Absorbance of Ursodeoxycholic acid was determined.

b.Calibration Curve of Ursodeoxycholic acid

A stock solution of 100mcg/ml of Ursodeoxycholic acid was prepared in methanol. For preparations of different concentrations,aliquots of stock solution were transferred into a series of 10 ml standard flasks and volumes were made with respective media.The different concentrations were prepared in the range of 2-25 mcg/ml of Ursodeoxycholic acid in distilled water for standard curve.

1.3.Formulation of Nanoparticles

Table 5.4 : Formulation plan for UDCA nanoparticles

INGREDIENTS	**FORMULATIONS**			
	F1	**F2**	**F3**	**F4**
Drug(mg)	45	45	45	45
Bovine Serum Albumin (mg)	45	90	135	180
Ethanol(ml)	10	10	10	10
Glutaraldehyde (%)	8	8	8	8
Mannose(mg) (coating agent)	20	20	20	20

1.3.1. Preparation of Bovine Serum Albumin nanoparticles from desolvation method

Bovine Serum Albuminnanoparticles were prepared by desolvation technique.The different amounts ofbovine serum albumin (i.e 45, 90, 135, 180 mg) weredissolvedin2.0 ml of 10mMNaCl solution, respectively, titrated to pH 8. The specified amount of drug was then added intobovine serum albumin solutions followed by the continuous addition of 8.0 ml of the desolvatingagent i.e. ethanol under stirring (500 rpm) at room temperature. After the desolvation process, few ml of 8% glutaraldehyde in water was added to induce particle crosslinking. The crosslinking process was performed under stirring of the suspension over a time period of 24 h.

1.3.2. Purification ofBovine Serum Albumin nanoparticles

The resulting nanoparticles were purified by three cycles of differential centrifugation (10,000 rpm for10 min) and redispersion of the pellet to the original volume of10mM NaCl at pH values of 8, respectively. Each redispersion step was performed in an ultrasonication bath over 5 min.The solvent was removed and the nanoparticles were collected and stored in a refrigerator.

1.3.3. **Mannose coating of Nanoparticles**

20 mg of Mannose were added to 10 mg of bovine serum albuminloadednanoparticles which is dispersed in 5 mL acidic phosphate buffer saline (pH 5.0), and the mixture was then stirred at room temperature over-night. The resulting nanoparticles were purified by three cycles of differential centrifugation (10,000 rpm for 10 min) and followed by redispersion of the pellet to the original volume in 10mM NaCl at pH 8, respectively. Each redispersion step was performed in an ultrasonication bath over 5 min. The solvent was evaporated and the nanoparticles were collected and stored at 2-8^{o}C.

1.3.4.Characterization of Nanoparticles

The formulated nanoparticles were evaluated for particle size and shape,zeta potential,drug content uniformity, entrapment efficacy, drug loading, in-*vitro*drugrelease study, ex-vivo study.

1.4.1. Shape and Size

The morphology and size of plain and mannose-coated nanoparticles was determinedby Scanning electron microscopy (SEM).

1.4.2. Zeta potential:

The zeta potential and surface charge of nanoparticles was determined by the Zeta Potential Analyzers.The zeta potential of a nanoparticle is commonly used to characterize the surface charge property of nanoparticles.

1.4.3. Drug content uniformity

500 mg of nanoparticles were crushed in mortar and pestle. 10 mg of powder were taken and introduced in a 100ml volumetric flask. The nanoparticles were dissolved in phosphate buffer pH7.4 and make up the volume upto 100ml. The above solution was analyzed by UV spectrometer at 235 nm.

1.4.4. Entrapment efficiencyand Loadingefficiency:

500 mg of nanoparticles were crushed in mortar and pestle. 10 mg of powder were taken and introduced in a 100ml volumetric flask. The nanoparticles were dissolved in phosphate buffer pH7.4 and make up the volume up to 100ml. The above solution was analyzed by UV spectrometer at 235 nm.

The entrapment efficiency and drug loadingof the prepared nanoparticles was calculated by the formula:

Entrapment efficiency (%)= Theoretical drug-practical drug× 100
Theoretical drug

Drug Loading efficiency (%) = Amount of drug in nanoparticles × 100
Amount of drug loaded nanoparticles

1.5.5. Percentage Yield:

It is calculated to knowabout the efficiency of any method, thus it helps in selection of appropriate method of production.Practical yield was calculated as the weight of nanoparticles recovered from each batch in relation to the sum of starting material. It can be calculated using following formula:

Percentage yield = Practical yield × 100
Theoretical yield

1.5.6. *In- vitro*drug release:

*In-vitro*drug release study was carried out by Modified Diffusion Apparatus. The apparatus consists of a beaker containing 50 ml of phosphate buffer pH 7.4 maintained at 37^{o}C under mild agitation (50 rpm) using a magnetic stirrer acts as receptor compartment. An open -ended tube acts as donor compartment and the egg membrane was tied into upper part of the donor compartment. 10 mg of nanoparticleswere placed into the donor compartment over the membrane which was dipped in the receptor compartment consisting buffer. Then, the samples were taken at different time intervals from the receptor compartment and were analyzed by UV spectrometer at 235nm.

1.5.7. Mathematical modeling:

The data obtained from *in-vitro*release studies was treated by various conventional mathematical models (zero-order, first-order, Higuchi,Hixon -Crowell model and Korsmeyer- Peppas) to determine the release mechanism from the designed nanoparticle formulations. Selection of a suitable release model was based on the values of R (correlation coefficient), k (release constant) and n (diffusion exponent) obtained from the curve fitting of release data.

1.5.7.1. Zero-order model

Drug dissolution from dosage forms that do not disaggregate and release the drug slowly can be represented by the equation:

$$\mathbf{Q_0 - Q_t = K_0 t}$$

Rearrangement of equation yields:

$$\mathbf{Q_t = Q_0 + K_0 t}$$

Where, Q_t is the amount of drug dissolved in time t,

Q_0 is the initial amount of drug in the solution

K_0 is the zero order release constant expressed in units of concentration/time.

To study the release kinetics, data obtained from *in vitro*drug release studies were plotted asCumulative amount of drug released versustime.

Application: This relationship can be used to describe the drug dissolution of several types of modified release pharmaceutical dosage forms, as in the case of some transdermal systems, as well as matrix tablets with low soluble drugs in coated forms, osmotic systems, etc.

1.5.7.2. First order model

This model has also been used to describe absorption and/or elimination of some drugs, although it is difficult to conceptualize this mechanism on a theoretical basis. The release of the drug which followed first order kinetics can be expressed by the equation:

$$\mathbf{\log C = \log C_0 - Kt / 2.303}$$

Where, C_0 is the initial concentration of drug.

K is the first order rate constant, and t is the time.

The data obtained are plotted as log cumulative percentage of drug remaining *vs*. time which would yield a straight line with a slope of - K/2.303.

Application: This relationship can be used to describe the drug dissolution in pharmaceutical dosage forms such as those containing water-soluble drugs in porous matrices.

1.5.7.3. Higuchi model

This model is based on the hypotheses that (i) initial drug concentration in the matrix is much higher than drug solubility; (ii) drug diffusion takes place only in one dimension (edge effect must be negligible); (iii) drug particles are much smaller than system thickness; (iv) matrix swelling and dissolution are negligible; (v) drug diffusivity is constant; and (vi) perfect sink conditions are always attained in the release environment.

In a general way it is possible to simplify the Higuchi model as:

$$f\,t = Q = K_H \times t^{1/2}$$

Where, K_H is the Higuchi dissolution constant

The data obtained were plotted as cumulative percentage drug release versus square root of time.

Application: This relationship can be used to describe the drug dissolution from several types ofmodified release pharmaceutical dosage forms, as in the case of some transdermal systems and matrixtablets with water soluble drugs.

1.5.7.4. Hixson-Crowell model

Hixson and Crowell (1931) recognized that the particles regular area is proportional to the cuberoot of its volume. They derived the equation:

$$W_O - W_t^{1/3} = kt$$

Where, W_0 is the initial amount of drug in the pharmaceutical dosage form.

W_t is the remaining amount of drug in the pharmaceutical dosage form at time t.

And k(kappa) is a constant incorporating the surface-volume relation. The equation describes the release from systems where there is a change in surface area and diameter of particles or tablets .To study the release kinetics, data obtained from *in vitro* drug release studies were plotted as cube root of drug percentage remaining in matrix versustime.

Application: This expression applies to pharmaceutical dosage form such as tablets, where the dissolution occurs in planes that are parallel to the drug surface if the tablet dimensions diminish proportionally,in such a manner that the initial geometrical form keeps constant all the time.

1.5.7.5. Korsmeyer-Peppas model

Korsmeyer et al. (1983) derived a simple relationship which described drug release from a polymeric system equation.To find out the mechanism of drug release, first 60% drug release data were fitted in Korsmeyer-Peppas model :

$$M_t / M_\infty = Kt^n$$

Where M_t / M_∞ is a fraction of drug released at time t,

K is the release rate constant and n is the release exponent.

The n value is used to characterize different release for cylindrical shaped matrices.In this model, the value of ncharacterizes the release mechanism of drug as described in table to study the release kinetics, data obtained from *in vitro*drug release studies wereplotted as log cumulative percentage drug release versuslog time.

Table 5.5: Interpretation of diffusional release mechanisms from polymeric films.

Release exponent (n)	Drug transport mechanism
0.5	Fickian diffusion
0.45 < n = 0.89	Non -Fickian transport
0.89	Case II transport
Higher than 0.89	Super case II transport

1.5.8.: Ex-vivo Study

Here cold trypsinisation method has been used in which a Goat liver was excised into small pieces and 200mg of tissue was rinsed with phosphate buffer saline. Then trypsin solution has been prepared and this solution is added to the tissues and kept in refrigerators for 12 hrs. so that proteolysis occurs and liver cells get separated. Now 10 mg of nanoparticles were added and left for few minutes so that binding of mannose to its receptors can take place.

After this the solution has been centrifuged and large tissues are separated and the decanted solution is kept and proper dilutions are made. Then, the samples were taken at definite time intervals from the receptor

compartment and were analyzed by UV spectrometer at 235 nm and unbound drug concentration can be easily calculated.

RESULTS AND DISCUSSIONS

Four formulations of Ursodeoxycholic acid were formulated using different drug polymer ratios. The formulation is subjected to evaluation parameters like particle size,zeta potential, drug content uniformity, percentage yield, entrapment efficiency, drug loading efficiency, *in-vitro* drug release study and Ex-vivo study.

6.1. Preformulation Studies

6.1.1. Identification of drug by FTIR:

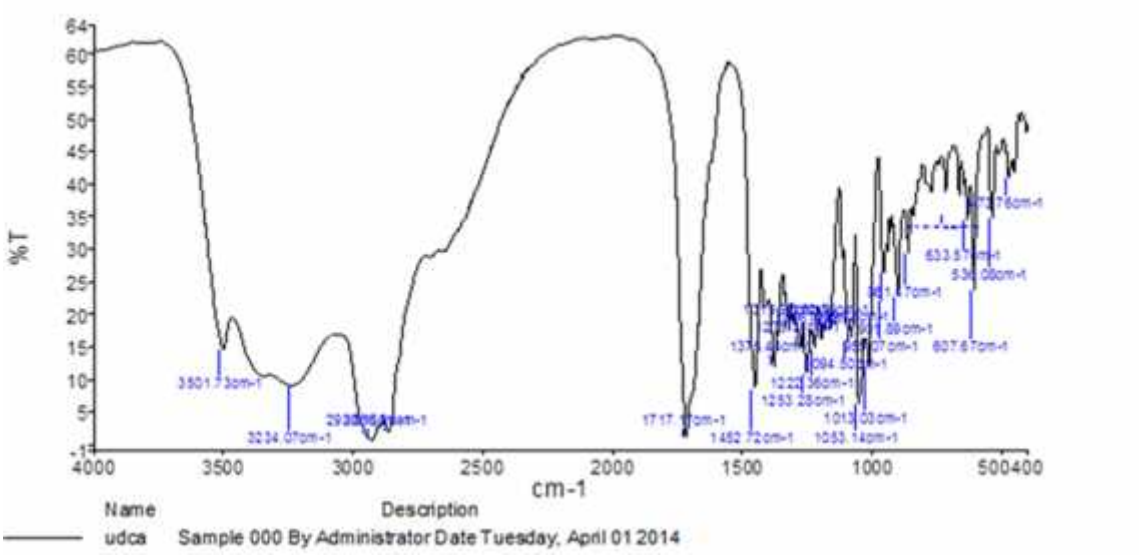

Fig 6.1: FTIR spectrum of Ursodeoxycholic acid

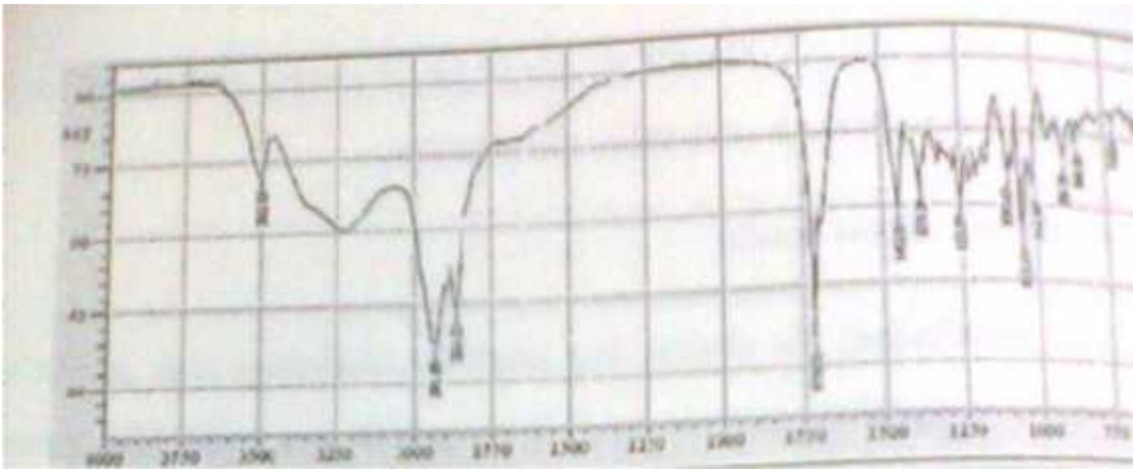

Fig 6.2.: FTIR spectrum of Ursodeoxycholic acid(with reference from B.P. 2010).

Table 6.1:Characteristics peaks of Ursodeoxycholic acid

S.No.	Reference peaks(cm^{-1})	Obtained Peaks (cm^{-1})	Functional Group	Stretching/Bending
1.	3500	3501	-OH (free)	Stretching

2.	3200	3234	-OH (H-bonded)	Stretching
3.	2850	2923	$-CH_3$	Stretching
4.	1700	1717	C=O	Stretching
5.	1400	1452	C=C	Stretching
6.	-	2930	-C-H (aromatic)	Stretching

The comparison between the peaks of two graphs shows that the characteristics peaks of Ursodeoxycholic acid(taken from I.P.) was found similar to the given drug sample, which shows that the drug is Ursodeoxycholic acid.

.**6.1.2.Organoleptic characteristics**:

The color,odor and taste of the drug were characterized and recorded using descriptive terminology, the results are shown in Table No. : 6.2.

Table 6.2: Results of Organoleptic properties.

S.No.	Properties	Results
1.	Description	Amorphous powder
2.	Color	White or almost white powder
3.	Odor	Characteristics
4.	Taste	Bitter

6.1.3. **Solubility:**

Ursodeoxycholic acid is freely soluble in acids, very slightly soluble in water, freely soluble in alcohol and soluble in phosphate buffer pH 7.4 as shown in Table No :6.3.

Table 6.3: Results of Solubility studies

S.No.	Solvent	Solubility	Solubility (mg/ml)
1.	Water	Very slightly soluble	20
2.	Acetone	Slightly Soluble	30
3.	Alcohol	Freely Soluble	10
4.	Glacial acetic acid	Freely Soluble	1

6.1.4. Melting Point determination:

The melting point of Ursodeoxycholic acidwas found to be 202-206°C.This value is same as that of the literature citation of 203° C.

Table 6.4: Results of Melting Point determination

Reported melting point	202-206°C
Observed melting point	203°C

6.2. Spectral Studies

6.2.1.Drug - excipient Compatibility Study:

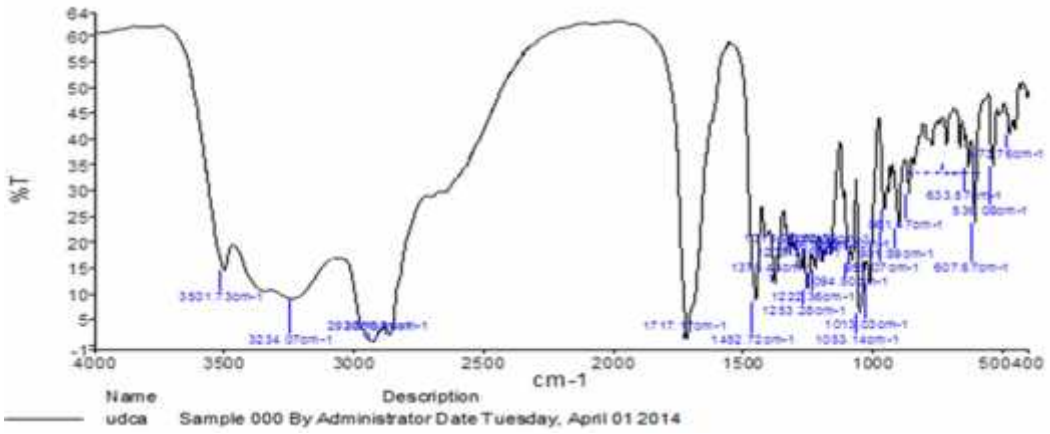

Fig 6.3: FTIR spectrum of Ursodeoxycholic acid

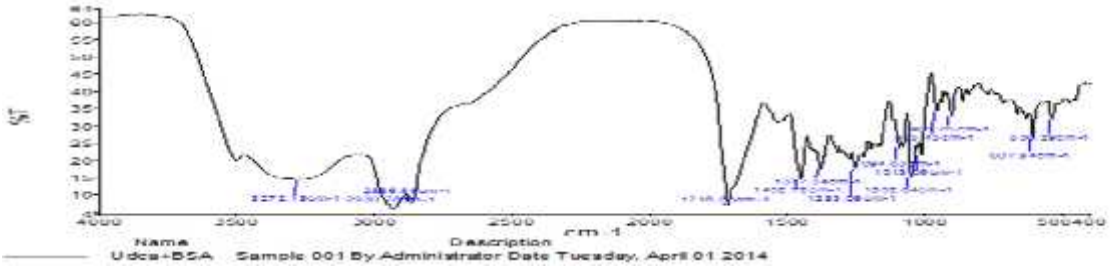

Fig 6.4. : FTIR spectrum of Ursodeoxycholic acid + Bovine Serum Albumin (polymer)

Table 6.5: Characteristics peaks of Ursodeoxycholic acid and Bovine Serum Albumin physical mixture

S.No.	Peaks(cm^{-1}) of drug	Peaks (cm^{-1}) of drug+ BSA	Functional Group	Stretching/Bending
1.	3501	3272	-OH (free)	Stretching
2.	3234	2930	-OH (H-bonded)	Srtetching
3.	2923	2866	$-CH_3$	Stretching
4.	1717	1716	C=O	Stretching
5.	1452	1452	C=C	Stretching
6.	2930	2930	-C-H (aromatic)	Stretching

The drug-polymer interactions shows that there was no major shifts in the absorption bands(peaks) of in presence of polymer and it was observed that all the characteristics peaks of drug is present in the combination of drug and polymer spectra indicating the compatibility of drug with the polymer used.

6.2.2. Preparation of Calibration Curve of Ursodeoxycholic acid

Determination of λ_{max} of Ursodeoxycholic acid:

UV absorption spectrum showed λ_{max} to be 235nm. The graph of absorbance V/s concentration for Ursodeoxycholic acidwas found to be linear in the concentration range of 2-25mcg/ml at 235 nm. Hence, the drug obeys Lambert-beer's law in this range. Fig.6.5shows UV spectrum of Ursodeoxycholic acid and Fig. 6.6. showsthe calibration curve of Ursodeoxycholic acid in ethanol and water.

The calibration curve was prepared and results were shown in Table 6.6.

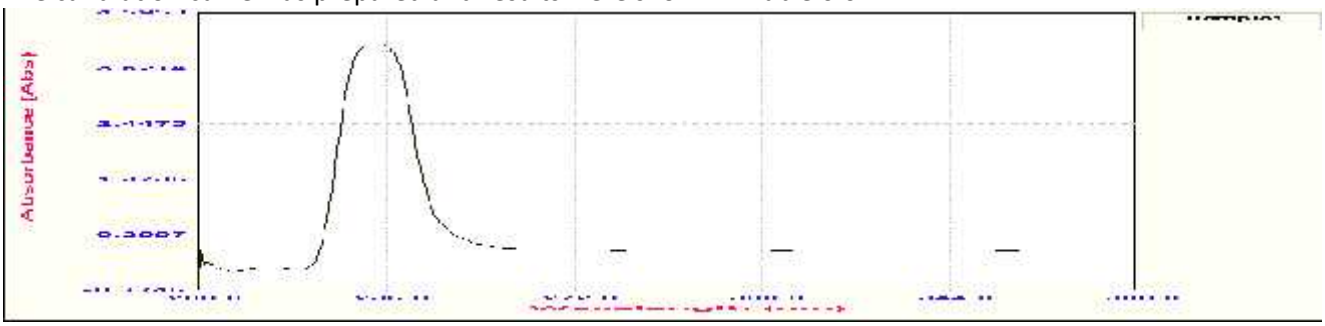

Fig 6.5.: UV Spectrum of Ursodeoxycholic acid

Wavelength of maximum absorption (λ_{max}) in distilled water was found to be 235nm.

Table6.6:Data for Calibration Curve of Ursodeoxycholic acid in distilled water

S.No.	Conc.(mcg/ml)	Absorbance(λ=235nm)
1.	**0**	**0**
2.	**2.5**	**0.1730**
3.	**5.0**	**0.2777**
4.	**10.0**	**0.3950**
5.	**15.0**	**0.5768**
6.	**20.0**	**0.7552**
7.	**25.0**	**0.9328**

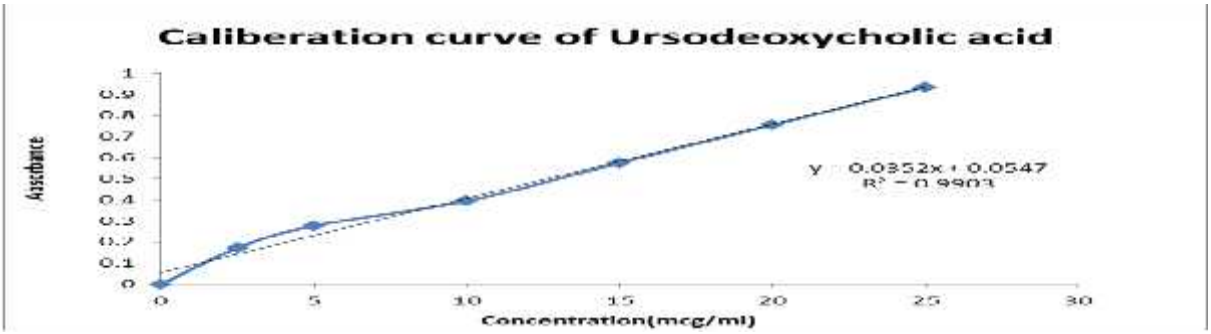

Fig. 2.6.: Calibration Curve of Ursodeoxycholic acid.

Line of Equation: y = 0.0352x+ 0.0547

Beer's Range: 2-25 mcg/ml

R^2 Value: 0.9903

λ max: 235nm

Fig.2.6 shows the calibration curve with slope 0.0352 and regression value 0.9903

6.3. Characterization of Nanoparticles

6.3.1. Particle Size

The SEM photomicrographs of nanoparticles are shown in Figs.6.7.Fig.(A,B,C,D) shows the Scanning electron microscopy (SEM) photomicrograph of albumin nanoparticles at different magnifications (2KX,500X,5.00KX,11.97KX) while fig.(C&D) shows the(SEM) photomicrograph of plain albumin nanoparticlesand mannose coated nanoparticles at magnification of 15.00 KX**.**

The particle size of plain nanoparticles was found to be in the size range of 200-800 nm and that of mannose coated nanoparticles was found to be in the size range of 250-850 nm.

It was observed from these photomicrographs that all samples of particles were smooth, sub-spherical in shape and aggregated to form small clusters.

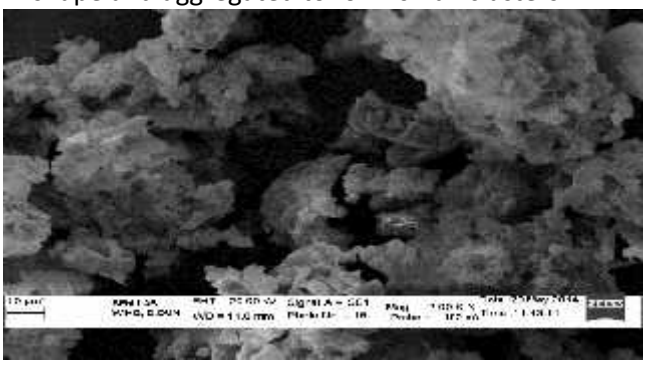

(A)

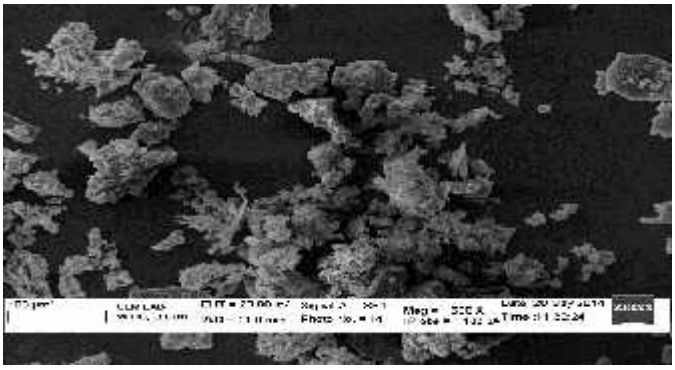

(B)

Fig.6.7:(A) Scanning electron microscopy (SEM) photomicrograph of Albumin nanoparticles at 2.00 KX . (B) SEM photomicrograph of Albumin nanoparticles at 500X.

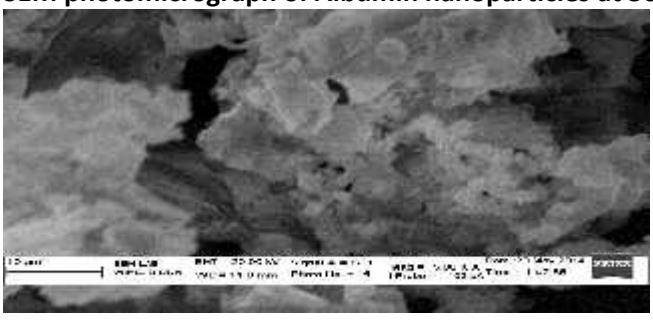

(C)

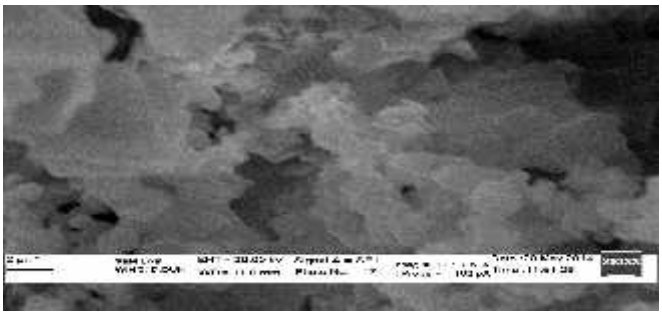

(D)

Fig.6.7:(C) Scanning electron microscopy (SEM) photomicrograph of Albumin nanoparticles at 5.00KX . (D) SEM photomicrograph of Albumin nanoparticles at 11.97KX.

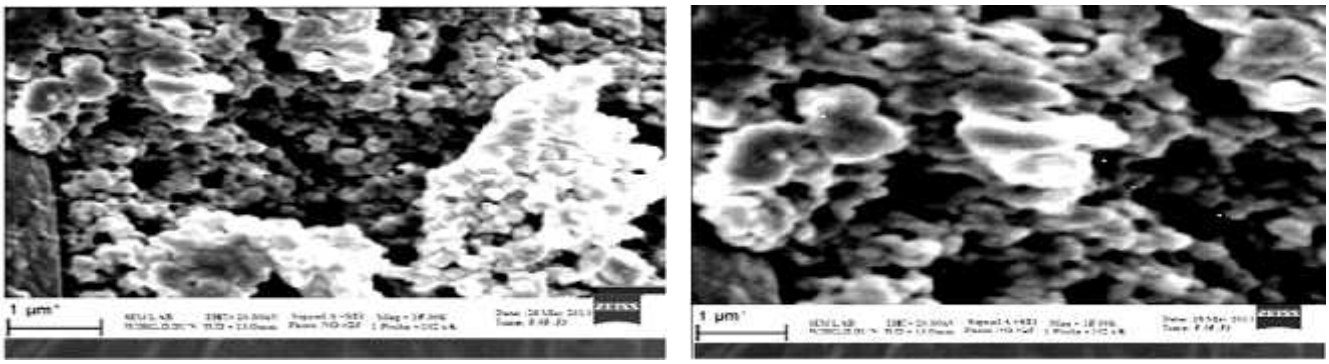

(E) **(F)**

Fig.6.7:(E) Scanning electron microscopy (SEM) photomicrograph of Albumin nanoparticles at 15.00 KX (F) SEM photomicrograph of mannose-6-phosphatecoated Albumin nanoparticles at 15.00 KX.

The larger particle size of mannose-6-phosphate nanoparticles as compared to plain nanoparticles could be due to the anchoring of mannose molecule at the surface of nanoparticles and hence an increment in size of nanoparticles was observed.

6.3.2. Zeta Potential

The graphs of zeta potential of plain and mannose-6-phosphate coated nanoparticles are shown in Figs 6.8(a & b).Thezeta potential of plain nanoparticles was found to be-3.61 and that of mannose-6-phosphate coated nanoparticles was found to be 64.1.

Theeffects of zeta potential on stability of the colloid are shown inTable 6.7.

Table 6.7: Effect of Zeta Potential on stability of the colloid

S.No.	Zeta potential [mV]	Stability behavior of the colloid
1.	From 0 to ±5	Rapid coagulation or flocculation
2.	From ±10 to ±30	Incipient instability
3.	From ±30 to ±40	Moderate stability
4.	From ±40 to ±60	Good stability
5.	More than ±61	Excellent stability

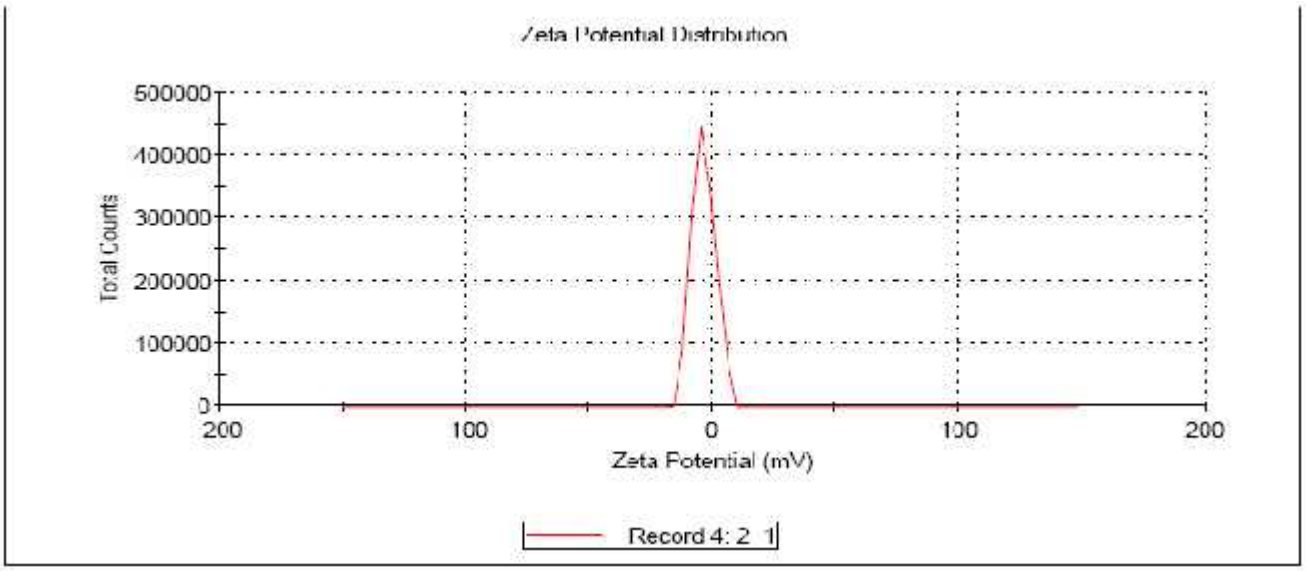

Fig.6.8 :(a)Zeta Potential of plain albumin nanoparticles

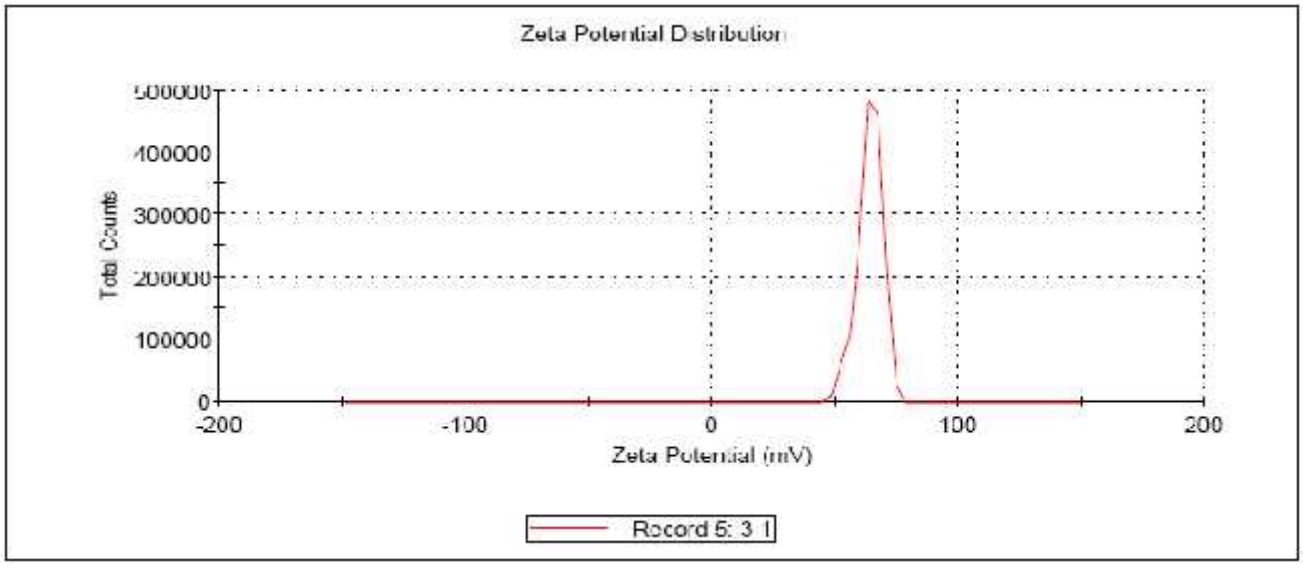

Fig.6.8 :(b) Zeta Potential of mannose-6-phosphate coated nanoparticles

The plain nanoparticles were negatively charged at pH 8. The low value of zeta potential shows the presence of flocs in nanoparticles which leads to the rapid coagulation of particles.Moreover, coating with mannose-6-phosphate makes the nanoparticles positively charged and also increases the zeta potential of nanoparticles and thus the nanoparticles shows the excellent stability after coating.

6.3.3. Drug content uniformity

The drug content of different formulations F1 to F4 was calculated and the content was found to be in range of 19.51 to 27.09 % for coated nanoparticles.The maximum drug content was found to be 27.09± 0.5% for coated nanoparticles in formulation F3.The results are shown in Table 6.8. Comparison of drug content for formulations F1 to F4 is shown in Fig.6.9. The reason of low drug content was due to drug partitioning to the external aqueous phase during formulation, which also leads to the low drug loading efficiency.

Table6.8: Drug Content of Plain and mannose-6-phosphate coated Ursodeoxycholic acid nanoparticles(for n =3)

Drug Content (%) ± S.D.	
Formulation Code	**Coated Nanoparticles**
F1	21.76 ± 0.63
F2	22.80 ± 0.71
F3	27.09 ± 0.5
F4	19.51 ± 0.62

6.3.4. Entrapment efficiency and Drug loading efficiency

The encapsulation efficiencies of all four formulations were given in the Table 6.9 and the entrapment efficiency was found to be 84.62 to 91.75 % for coated nanoparticles.Comparison of entrapment efficiency for formulations F1 to F4 is shown in Fig. 6.10. The maximum entrapment efficiency was found to be 91.75 ± 0.59 % for the formulation F3.The entrapment efficienciesof nanoparticles are larger than 80%,the drug can be effectively loaded inside the nanoparticles.The encapsulation efficiency increases with increasing polymer concentration upto a certain ratio.

The relatively higher percent drug entrapment was obtained which could be due to minimum repulsion between drug and polymer.

Table 6.9: Entrapment efficiency of Plain and mannose coated Ursodeoxycholic acid nanoparticles (for n =3)

Entrapment efficiency (%) ± S.D.	
Formulation Code	**Coated Nanoparticles**
F1	84.62 ± 0.37
F2	88.75 ± 0.46
F3	91.75 ± 0.59
F4	83.98 ± 1.10

Drug loading efficiency

Thedrug loadingefficiency of all four formulations were given in the Table 6.10and it was found to be in range of 3.80 to 19.08 % for coated nanoparticles.Comparison of entrapment efficiency for formulations F1 to F4 is shown in Fig.6.11.The maximum drug loading efficiency was found to be 19.08% ± 1.10 in coated nanoparticles for formulation F4 .

Loading efficiency may be increased by increasing the polymer ratio, so that sufficient quantity of polymer will be able to entrap the drug present in solution.

The main reason for low drug loading efficiency was low drug-polymer binding.The drug has low protein binding therefore; most of the drug can easily diffuse through the matrix.

Further, the existing albumin-based drug delivery systems are often limited by their low drug loading capacity as well as noticeable drug leakage into the blood circulation.

Table 6.10 :Drug Loading efficiencyof mannose coated Ursodeoxycholic acid nanoparticles (for n =3)

Drug Loading efficiency (%)± S.D.	
Formulation Code	**Coated Nanoparticles**
F1	3.80 ± 0.45
F2	7.67 ± 0.79
F3	18.09 ± 0.9
F4	19.08 ± 1.10

6.3.5. Percentage Yield

The percentage yields of different formulations F1 to F4 were calculated and the yield was found to be in the range of 25.98 to 62.32% for coated nanoparticles.Percentage yield of all batches is shown in Table 6.11.Comparison of percentage yield for formulations F1 to F4 is shown in Fig.6.12.The maximum percentage yield was found to be 62.32% for coated nanoparticles in formulation F4, where the concentration of albumin is highest while the nanoparticleyield is lowest in F1 i.e. 25.98 % where the concentration of albumin is lowest.

The reduction in percentage yield after coating of nanoparticles might be occur due to the loss of nanoparticles during the coating process.

Table 6.11 : Percentage Yield of mannose coated Ursodeoxycholic acid nanoparticles

Formulation Code	**Total amount of ingredients (mg)**	**Percentage Yield (%)**
	Coated Nanoparticles	**Coated Nanoparticles**
F1	110	25.98
F2	155	37.09
F3	200	46.72
F4	245	62.32

6.3.6. *In-vitro*drug release:

The dissolution study on all four formulations of Ursodeoxycholic acid was carried out in phosphate buffer pH 7.4 buffer using egg membrane and modified apparatus.The *in-vitro* drug release of all four formulations F1 to F4 are shown in Table 6.12.The cumulative percentdrug release after 10 hrs was found to be between 51.78% to 35.01 % for formulations F1 to F4 respectively. From the results, it was concluded that increase in polymer concentration, decreases the drug releases from the nanoparticles**.**

It was also found that coating of nanoparticles with mannose retard the rate of drug release as compared to plain nanoparticles.

Table 6.12: *In-vitro* release profile of Formulations F1 to F4 (mannose-6-phosphate coated Nanoparticles)

Time (hrs)	Cumulative % drug release			
	F1	**F2**	**F3**	**F4**
0	0	0	0	0
1	13.31	17.46	11.08	9.11
2	21.36	25.64	18.04	16.45
3	27.99	31.20	24.39	22.44
4	32.20	36.11	29.50	27.02
5	36.34	40.65	33.02	31.69
6	39.54	43.62	36.44	34.02
7	42.33	46.33	39.36	37.38
8	44.32	48.01	42.61	40.02
9	46.92	49.03	43.06	42.01
10	47.23	49.62	44.31	43.21

Table 6.13:*In-vitro* release profile of Ursodeoxycholic acid from Formulations F1

Time (hrs)	√T	Log T	% CDR	%Cumulative drug remained	Log % CDR	Log %Cumulative drug remained
0	0	-	0	100	-	2
1	1	0	13.31	86.69	1.124	1.937
2	1.414	0.3	21.36	78.64	1.329	1.895
3	1.732	0.47	27.99	72.01	1.447	1.857
4	2	0.6	32.20	67.8	1.507	1.831
5	2.236	0.69	36.34	63.66	1.560	1.803
6	2.449	0.77	39.54	60.46	1.597	1.781
7	2.645	0.84	42.33	57.67	1.626	1.760
8	2.828	0.9	44.32	55.68	1.646	1.745
9	3	0.95	46.92	53.08	1.671	1.724
10	3.162	1	47.23	52.77	1.674	1.722

Table 6.14: *In-vitro* release profile of Ursodeoxycholic acid from Formulations F2

Time (hrs)	√T	Log T	% CDR	%Cumulative drug remained	Log % CDR	Log %Cumulative drug remained
0	0	-	0	100	-	2
1	1	0	17.46	82.54	1.242	1.916
2	1.414	0.3	25.64	74.36	1.408	1.871
3	1.732	0.47	31.20	68.8	1.494	1.837

4	2	0.6	36.34	63.89	1.557	1.805
5	2.236	0.69	40.65	59.35	1.609	1.773
6	2.449	0.77	43.62	56.38	1.639	1.751
7	2.645	0.84	46.33	53.67	1.665	1.729
8	2.828	0.9	48.01	51.99	1.681	1.715
9	3	0.95	49.03	50.97	1.609	1.707
10	3.162	1	49.62	50.38	1.695	1.702

Table 6.15 : *In-vitro* release profile of Ursodeoxycholic acid from Formulations F3

Time (hrs)	**√T**	**Log T**	**% CDR**	**%Cumulative drug remained**	**Log % CDR**	**Log %Cumulative drug remained**
0	0	-	0	100	-	2
1	1	0	11.08	88.92	1.044	1.942
2	1.414	0.3	18.04	81.96	1.256	1.913
3	1.732	0.47	24.39	75.61	1.387	1.878
4	2	0.6	29.50	70.5	1.498	1.848
5	2.236	0.69	33.02	66.98	1.518	1.825
6	2.449	0.77	36.44	63.56	1.561	1.803
7	2.645	0.84	39.36	60.64	1.595	1.782
8	2.828	0.9	42.61	57.39	1.629	1.758
9	3	0.95	43.06	56.94	1.634	1.755
10	3.162	1	43.31	55.69	1.646	1.745

Table 6.16: *In-vitro* release profile of Ursodeoxycholic acid from Formulations F4

Time (hrs)	**√T**	**Log T**	**% CDR**	**%Cumulative drug remained**	**Log % CDR**	**Log %Cumulative drug remained**
0	0	-	0	100	-	2
1	1	0	9.11	90.89	0.959	1.958
2	1.414	0.3	16.45	83.55	1.216	1.921
3	1.732	0.47	22.44	77.56	1.351	1.889
4	2	0.6	27.02	72.98	1.431	1.863
5	2.236	0.69	31.69	68.31	1.50	1.834
6	2.449	0.77	34.02	65.98	1.531	1.819
7	2.645	0.84	37.38	62.62	1.572	1.796

8	2.828	0.9	40.02	59.98	1.602	1.778
9	3	0.95	42.01	57.99	1.623	1.763
10	3.162	1	43.21	56.79	1.635	1.754

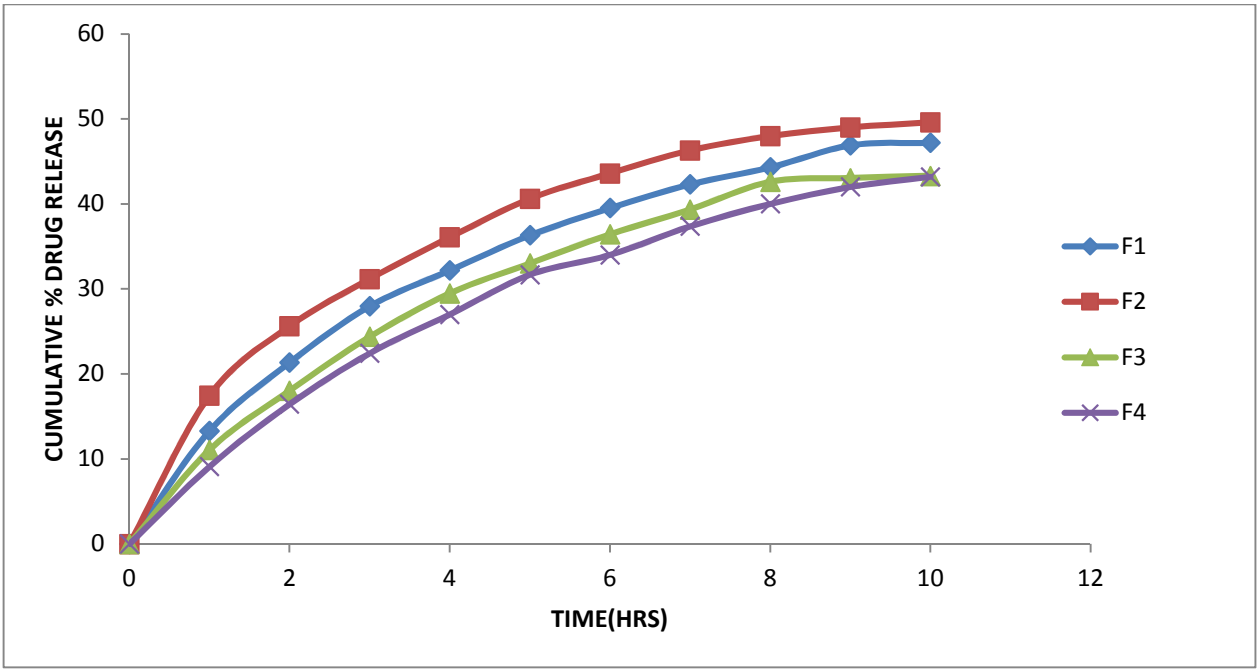

Fig 6.13 :Zero order release Plot of Ursodeoxycholic acid nanoparticles

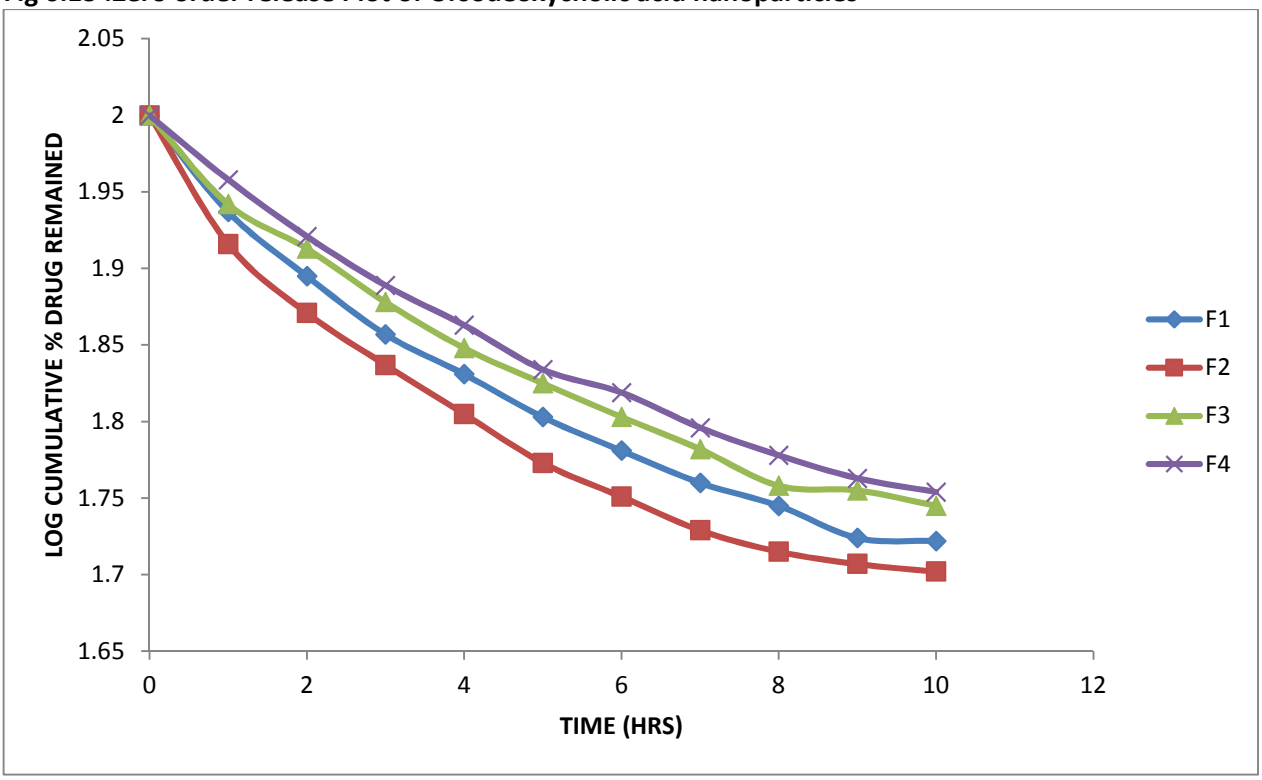

Fig. 6.14:First order release Plot of Ursodeoxycholic acid nanoparticles

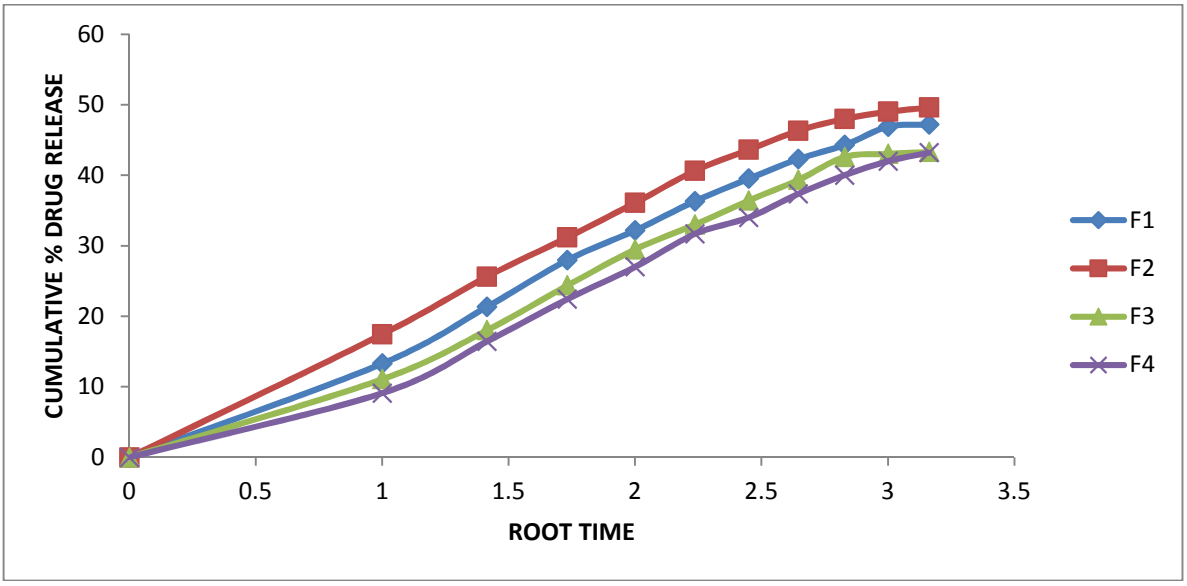

Fig.6.15:Higuchi Plot of Ursodeoxycholic acid nanoparticles

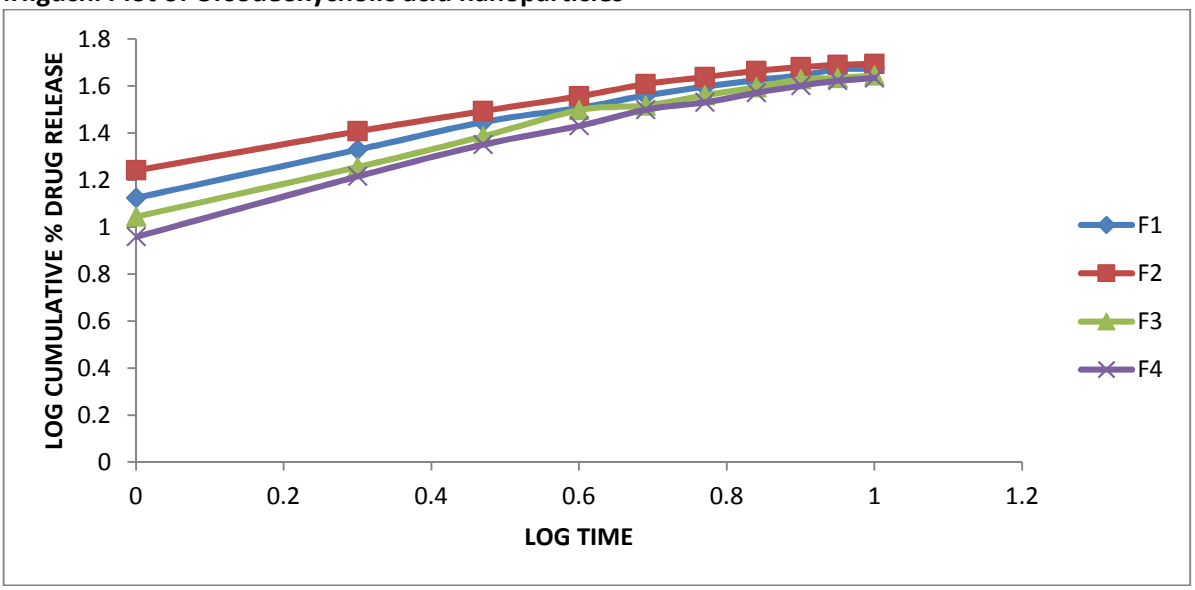

Fig.6.16:KorsmeyerPeppa's Plot of Ursodeoxycholic acid nanoparticles

6.3.7. Mathematical modeling:

The data obtained from *in-vitro* release studies was treated by various conventional mathematical models (zero-order, first-order, Higuchi and Korsmeyer- Peppa's) to determine the release mechanism from the designed nanoparticle formulations. Selection of a suitable release model was based on the values of R (correlation coefficient), k (release constant) and n (diffusion exponent) obtained from the curve fitting of release data.

In-vitro drug release dataof all four formulations F1 to F4 are shown in Table 6.12.

The regression coefficients of the all formulations F1 to F4 are shown in Table 6.17.

It was found that all the formulations follows the first order kinetics.

The regression coefficients for the formulations F1 to F4 of Higuchi plot was found to be almost linear.The linearity suggests that the release ofUrsodeoxycholic acid nanoparticles was diffusion controlled.

Korsmeyer- Peppas release model is widely used when the release mechanism is not well known or when more than one type of release phenomenon could be involved.The value of n could be used to characterize different release mechanism.The value of n for F1 to F4 was found to be respectively greater than 0.8.The formulations F1 and F2 indicate that the release approximates non-Fickian diffusion mechanism while the formulations F3 and F4 shows the Super Case-II transport mechanism.

Table 6.17: Model fitting release profile of Formulations F1 to F4

Formula-tion Code	Regression Coefficient (R^2)			Slope (n) value
	Zero order	First order	Higuchi's	Korsmeyer- Peppas
F1	0.897	0.944	0.992	0.551
F2	0.852	0.912	0.985	0.462
F3	0.909	0.953	0.987	0.608
F4	0.935	0.967	0.988	0.672

6.3.8. Selection of ideal batch:

Among the different Ursodeoxycholic acid nanoparticles formultions, the formulation F3 was selected as the ideal formulation after considering its optimum particle size, zeta potential, percentage yield, drug content, entrapment efficiency and also drug release at sustained manner upto 10 hrs.

6.3.9. Receptor-ligand binding study:

From the study, it was found that the amount of dug release from the formulation F3 after 10 hrs was only 5.67%, prior to that the release was 42.09%.So, the remaining 36.42% drug binds with receptor present in hepatocytes.

CONCLUSIONS

In the present study, an attempt was made to develop mannose -6- phosphate coated albumin nanoparticles of Ursodeoxycholic acid for the treatment of Cirrhosis with a view to provide targeted action to the required site and achieve therapeutic efficacy.

From the results it can be concluded that:

- Nanoparticles were successfully prepared by desolvation method. The method was able to produce discrete, free-flowing nanoparticles.
- Bovine serum Albumin is a biocompatible and biodegradable polymer for preparing targeted nanoparticles.
- FTIR was carried out to find out the possible interaction between the drug and polymer. The study revealed that there was no interaction between the drug and polymer.
- The particle size analysis revealed that particle size were found in the range of 200-800 nm for plain nanoparticles and 250-850 nm for coated nanoparticles.
- The zeta potential of plain nanoparticles were found to be -3.61 and that of mannose coated nanoparticles was found to be 64.1. The low value of zeta potential shows the presence of flocs in nanoparticles which leads to the rapid coaugulation of particles. Moreover, coating with mannose makes the nanoparticles and thus the nanoparticles and thus the nanoparticles shows the excellent stability after coating.
- From in-vitro studies, it was concluded that increase in polymer concentration, decreases the drug release from the nanoparticles.
- From the percent yield, it was concluded that the maximum percentage yield was found to be 62.32% in the formulation F4, where the concentration of albumin is highest while the nanoparticle yield is lowest in F1 i.e.25.98 % where the concentration of albumin is lowest.
- The maximum entrapment efficiency was found to be 91.75±0.59 in formulation F3. The entrapment efficiency are larger than 80%, the drug can be effectively loaded inside the nanoparticles.
- The maximum drug loading efficiency was found to be 19.08± 1.10 in formulation F4. Loading efficiency may be increased by increasing the polymer ratio, so that sufficient quantity of polymer will be able to entrap the drug present in solution.
- The maximum drug content was found to be 27.09±0.5 in the formulation F3. The reason of low drug content was low drug loading.
- From the ex-vivo study it was found that the amount of free drug in F2 formulation after the 10 hrs was only 8.34% having its % CDR is 49.62 means remaining 40.28 get attached to the liver cells.

ACKNOWLEDGEMENT

Author would like to thank Dr. (Prof.) Preeti Kothiyal and Dr. Ganesh Bhatt for their guidance and moral support during research work.

REFERENCES

1. Bataller R and Brenner D (2005). Liver fibrosis. J. Clin. Invest., 115:209-218.
2. Beljaars L et al. (1999). Albumin modified with mannose 6-phosphate: A potential carrier for selective delivery of antifibrotic drugs to rat and human hepatic stellate cells. Hepatol. 29:1486-1493.
3. Bataller R and Brenner D (2006). Hepatic stellate cells as a target for the treatment of liver fibrosis. Semin. Liver Dis. 21:437-451.
4. Friedman S.L (2006).The virtuosity of hepatic stellate cells. Gastroenterology. 117:1244-1246
5. Friedman S.L (2003). Liver fibrosis – from bench to bedside. J. Hepatol. 38 Suppl 1:S38-S53.
6. Neff et al. (2011).The Current Economic Burden of Cirrhosis. Vol. 7. Gastroenterology & Hepatology.
7. Friedman S L (2008). Hepatic Stellate Cells: Protean, Multifunctional, and Enigmatic Cells of the Liver. Physiol. Rev 88: 125–172.
8. Bal W et al. (1998). Multi-metal binding site of serum albumin. J. Inorg. Biochem. 70:33-39.
9. De Bleser et al. (1995). A Insulin like growth factor-II/mannose 6-phosphate receptor is expressed on CCl_4-exposed rat fat-storing cells and facilitates activation of latent transforming growth factor-β in cocultures with sinusoidal endothelial cells. Hepatol 21:1429-1437.
10. Moreno M et al. (2010). Reduction of advanced liver fibrosis by short-term targeted delivery of an angiotensin receptor blocker to hepatic stellate cells in rats. Hepatology; 51:942-52.
11. Beljaars L et al. (2001) Characteristics of the hepatic stellate cell-selective carrier mannose 6-phosphate modified albumin(M6P(28)-HSA). Liver;21:320-8.
12. K. Poelstra et al. (2012). Drug targeting to the diseased liver. Journal of Controlled Release 161 188–197.
13. Zhipeng et al. Novel materials which possess the ability to target liver cells. http://www.paper.edu.cn.
14. Beljaars et al. (2000) Successful Targeting to Rat Hepatic Stellate cells using albumin HKmodified with cyclic Peptides That Recognize the Collagen Type VI Receptor. J. Biol. Chem. Vol. 275, No. 17.
15. Beljaar L et al. (1999). Albumin modified with mannose 6-phosphate: A potential carrier for selective delivery of antifibrotic drugs to rat and human hepatic stellate cells. Hepatol 29:1486-1493.
16. Wu J and Zern M. A. (2000). HSC: target for liver fibrosis treatment J Gastroenterol; 35:665–672.
17. Sato Y et al. (2008). Resolution of liver cirrhosis using vitamin A-coupled liposomes to deliver siRNA against a collagen-specific chaperone, Nat. Biotechnol. 26 431–442.
18. Wang L et al. (2006). Arg-gly-asp-mannose-6-phosphate inhibits activation and proliferation of hepatic stellate cells in vitro, World J.Gastroenterol. 12 1303–1307.
19. Elrick L et al. (2005). Generation of a monoclonal human single chain antibody fragment to hepatic stellate cells — a potential mechanism for targeting liver anti-fibrotic therapeutics. J. Hepatol. 42 888–896.
20. Adrian J.E et al. (2006). Interaction of targeted liposomes with primary cultured hepatic stellate cells: involvement of multiple receptor systems. J. Hepatol. 44 560–567.